

ADA030725

AFWL-TR-76-107

AFWL-TR-
76-107

A FEASIBILITY EXPERIMENT FOR A SOFT X-RAY LASER

September 1976

Final Report

Approved for public release; distribution unlimited.



OCT 14 1976


AIR FORCE WEAPONS LABORATORY
Air Force Systems Command
Kirtland Air Force Base, NM 87117

This final report was prepared by the Air Force Weapons Laboratory, Kirtland Air Force Base, New Mexico under Job Order 88091601. Captain Jerry Bettis (LRE) was the Laboratory Project Officer-in-Charge.

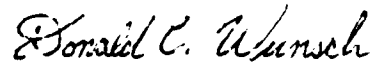
When US Government drawings, specifications, or other data are used for any purpose other than a definitely related Government procurement operation, the Government thereby incurs no responsibility nor any obligation whatsoever, and the fact that the Government may have formulated, furnished, or in any way supplied the said drawings, specifications, or other data is not to be regarded by implication or otherwise as in any manner licensing the holder or any other person or corporation or conveying any rights or permission to manufacture, use, or sell any patented invention that may in any way be related thereto.

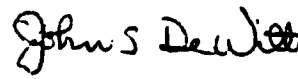
This report has been reviewed by the Information Office (OI) and is releasable to the National Technical Information Service (NTIS). At NTIS, it will be available to the general public, including foreign nations.

This technical report has been reviewed and is approved for publication.


JERRY R. BETTIS
Captain, USAF
Project Officer

FOR THE COMMANDER


DONALD C. WUNSCH
Acting Chief, Applied Research Branch


JOHN S. DeWITT
Lt Colonel, USAF
Chief, Technology Division

DO NOT RETURN THIS COPY. RETAIN OR DESTROY.

UNCLASSIFIED

SECURITY CLASSIFICATION OF THIS PAGE (When Data Entered)

REPORT DOCUMENTATION PAGE		READ INSTRUCTIONS BEFORE COMPLETING FORM
1. REPORT NUMBER 14 AFWL-TR-76-167	2. GOVT ACCESSION NO.	3. RECIPIENT'S CATALOG NUMBER 9
4. TITLE (and Subtitle) 6 A FEASIBILITY EXPERIMENT FOR A SOFT X-RAY LASER.		5. TYPE OF REPORT & PERIOD COVERED Final Report,
7. AUTHOR(s) 10 G. R. Doughty, Captain, USAF R. A. Wallner, Captain, USAF A. H. Guenther		6. PERFORMING ORG. REPORT NUMBER
9. PERFORMING ORGANIZATION NAME AND ADDRESS Air Force Weapons Laboratory (LRE) Kirtland Air Force Base, NM 87117		8. CONTRACT OR GRANT NUMBER(s)
11. CONTROLLING OFFICE NAME AND ADDRESS Air Force Weapons Laboratory Kirtland AFB, NM 87117		10. PROGRAM ELEMENT, PROJECT, TASK AREA & WORK UNIT NUMBERS 17 62601F 88091601 16 AF-8809
14. MONITORING AGENCY NAME & ADDRESS (if different from Controlling Office) 12 402		12. REPORT DATE 11 Sep 1976
		13. NUMBER OF PAGES 38
		15. SECURITY CLASS. (of this report) Unclassified
		15a. DECLASSIFICATION/DOWNGRADING SCHEDULE
16. DISTRIBUTION STATEMENT (of this Report) Approved for public release; distribution unlimited.		
17. DISTRIBUTION STATEMENT (of the abstract entered in Block 20, if different from Report)		
18. SUPPLEMENTARY NOTES		
19. KEY WORDS (Continue on reverse side if necessary and identify by block number) Laser X-Ray X-Ray Laser Plasma X-Rays		
20. ABSTRACT (Continue on reverse side if necessary and identify by block number) X-ray lasing in the region of 44 to 117 Å is possible using a mode-locked, picosecond Nd ³⁺ : glass laser as a pump. This report discusses the necessary conditions along with expected gain and loss mechanisms. Also detailed is a history of Air Force Weapons Laboratory involvement in this effort.		

DD FORM 1 JAN 73 1473

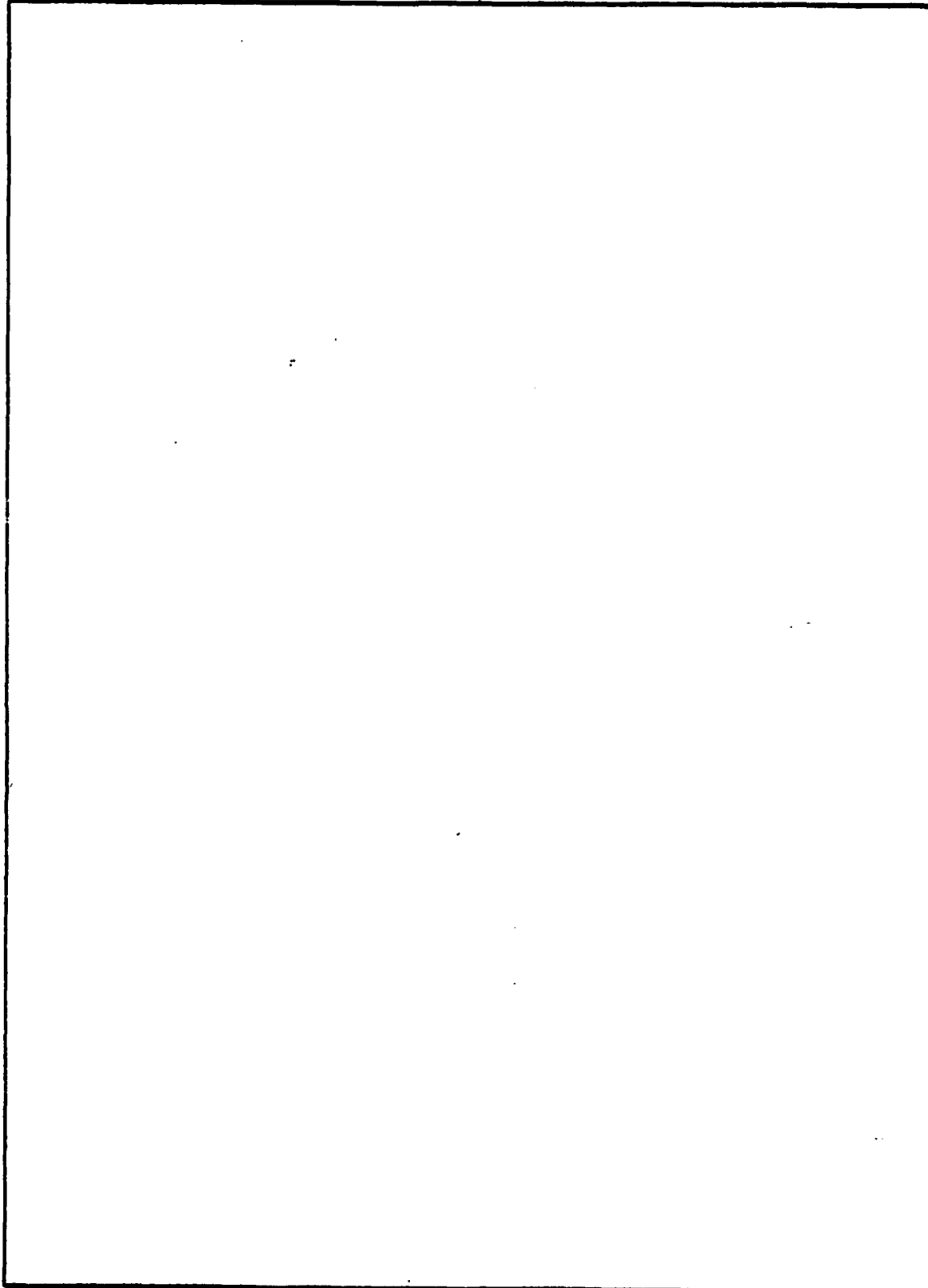
EDITION OF 1 NOV 68 IS OBSOLETE

UNCLASSIFIED

SECURITY CLASSIFICATION OF THIS PAGE (When Data Entered)

013 150

SECURITY CLASSIFICATION OF THIS PAGE(When Data Entered)



SECURITY CLASSIFICATION OF THIS PAGE(When Data Entered)

OCT 14 1976

CONTENTS

<u>Section</u>		<u>Page</u>
I	INTRODUCTION	1
	Synopsis	1
	Applications	1
	Historical Survey	3
II	TECHNICAL CONSIDERATIONS	6
	Introduction	6
	General Requirements for Laser Action	6
	Possible Approaches	6
	Electron Beams	7
	Ion Beams	7
	Mode-Locked Laser	8
	Selection of Approach	12
	Soft X-ray Laser	13
	Conclusions	17
III	THE PROGRAM	
	Introduction	18
	Verification of X-ray Laser Action	18
	Investigation of the Plasma/X-ray Parameters	19
	Plasma/X-ray Diagnostics	22
IV	HARD X-RAY LASERS	
	Introduction	29
	The Utah Experiment	29
	Other Hard X-ray Laser Considerations	29
V	SUMMARY	
	Conclusions	31
	Future Directions	31
	REFERENCES	33

ACCESSION for	
NTIS	White Section <input checked="" type="checkbox"/>
DDC	Ref Section <input type="checkbox"/>
UNANNOUNCED	<input type="checkbox"/>
JUSTIFICATION.....	
BY	
DISTRIBUTION AVAILABILITY CODES	
DATE	
A	

ILLUSTRATIONS

<u>Figure</u>		<u>Page</u>
1	Schematic Diagram of Target Design and Orientation	14
2	(a) Split-Beam Excitation for Determining Laser Action	20
	(b) Ratio of Detector of Signal No. 1 to Detector Signal No. 2 (Ordinate) versus Time Delay (Abscissa) Between Split Laser Beams.	20
3	Schematic Drawing of Soft X-ray Laser Experimental Chamber	23
4	Sketch of Vacuum Chamber	24

SECTION I

INTRODUCTION

1. SYNOPSIS

The purpose of this report is to present an analysis of an experiment to achieve a coherent, monochromatic X-ray pulse in the soft X-ray region and to determine its temporal, spatial, and spectral characteristics. Upon verification of X-ray lasing, it would be desirable to perform further experiments to determine and optimize the conditions required to achieve X-ray laser action.

A theoretical study (ref. 1) by personnel of the Air Force Weapons Laboratory (AFWL) and the National Magnetic Laboratory (NML) at the Massachusetts Institute of Technology indicated that a soft X-ray laser may be feasible using a high power mode-locked Nd: glass laser system for creating a population inversion in several materials. These calculations showed that a pulse of 10 to 20 joules in a pulse of 20 picoseconds width would be sufficient to create X-ray lasing in low Z targets.

2. APPLICATIONS

There are many significant technical applications for an X-ray laser. Of particular interest to the Air Force would be its use in simulation studies. An X-ray laser would be a valuable calibration source for numerous weapon, plasma, and simulator diagnostics. Such a calibration source would enable the precise evaluation of the wavelength sensitivity and response time of various detectors. In addition, the coherence of the X-ray beam would allow X-ray material interaction studies at sufficiently high powers without interference from the plasma debris which is present in other X-ray sources (dense plasma focus, etc.). The concentrated X-ray flux could also serve to delineate the effects of high energy solar flares or other soft X-radiation on satellites and their materials.

X-ray lasers would most certainly find significant and extensive application in the field of material science. It would be of obvious benefit to have a nearly monochromatic ultrahigh flux source in the X-ray region. Dynamic processes could, in effect, be temporarily frozen to elucidate the configuration and structural response of matter on a time resolved basis. Details of molecular and atomic structures as well as the production of defects and the influence of

dislocations could be investigated within a time frame of a few optical cycles or lattice vibrations. An X-ray laser would be a valuable analytical instrument in ESCA (Electron Scattering for Chemical Analysis). It could also be used as a source for freezing density profiles in shocked materials in equation of state determinations. With the advent of the X-ray laser, a whole new domain of material science investigations would be feasible.

Application of X-ray lasers to molecular and biological systems will depend on the properties of the actual devices. Structural determinations could possibly be made with X-ray holography and phase contrast microscopy as well as X-ray scattering data. It might even be possible for scientists to study changes in malignant cells during the different stages of development.

Medical studies would also be enhanced by the use of an X-ray laser. The variation of absorption of body components to X rays could allow for precise in situ observation of bodily functions. Eye surgery and remote internal surgery could conceivably be accomplished using a coherent X-ray beam.

In addition, the use of an X-ray laser will significantly increase the probability of observing light-on-light scattering in the laboratory. Since the cross section for such scattering has a λ^{-6} dependence, the short wavelength provided by an X-ray laser is extremely important. For example, at 1.06μ , the cross section for photon-photon interactions is 10^{-64} cm^2 , while at 10 \AA , the cross section is on the order of 10^{-46} cm^2 . This increase by a factor of 10^{18} could allow observation of photon-photon scattering in a laboratory environment when employing high power lasers.

Perhaps the greatest application will come in high time resolution X-ray photography. ERDA has embarked on a large scale laser fusion program initially aimed at achieving sufficient thermometric yield from a single pellet to initiate a fusion reaction. The successful demonstration of this feat will lead to something close to an ideal laboratory size nuclear weapon environment simulator for the irradiation of large scale systems. To realize this achievement with realistic amounts of laser energy (1 kJ-10 kJ), the ERDA is relying on inertial compression of the target by spherical irradiation. At present, there is no direct method of assessing the uniformity of the implosion. The short wavelength (10 to 50 \AA) of the proposed X-ray laser is ideally suited to evaluate the sphericity of 50 to 200μ sized targets.

It is also obvious that the first demonstration of an X-ray laser will be a lasting contribution to science.

3. HISTORICAL SURVEY

The AFWL has been interested in the development of an X-ray laser since 1971. At that time, Lax and Guenther published their initial paper (ref. 2) indicating some required conditions for achieving an X-ray laser. In 1972, funds were obligated to NML for an initial feasibility experiment. At the same time, AFWL was establishing the Large Neodymium Glass Laser (LNGL) facility. In addition to many other possible applications, the LNGL facility in its final intended state could be used to pump an X-ray laser. The year 1974 saw an end to both of the above efforts when funding was diverted to other projects at AFWL.

The obvious importance of this area of endeavor led other laboratories to make observations which relate to possible X-ray lasing; these include Battelle Memorial Institute (ref. 3), Lawrence Livermore Laboratory (ref. 4), Naval Research Labs (ref. 5), University of Paris (ref. 6), University of Utah (ref. 7), University of Arizona (ref. 8), and Stanford University (ref. 9). In particular, studies of X-ray emission from laser produced plasmas at the Lebedev Institute (ref. 10), Culham Laboratories (ref. 11), and University of Paris (ref. 6) have produced important results in this area.

Mallozzi (ref. 12), at Battelle, has reported efficient generation of broadband X rays from various laser plasmas. He explored a number of target geometries and conditions to determine the variations in conversion efficiency (1.06 μ laser energy to X-radiation) for various high Z materials (iron, lead, gold, aluminum). The report suggests that 10 to 20 percent of the incident laser energy can be converted to X rays below 1 keV.

A Lawrence Livermore Laboratory report (ref. 13) indicates the production of a thermal Bremsstrahlung continuum as well as a line emission character for gold targets at about 2.4 and 3.5 keV. These very intense signal line emissions suggest the possibility of a stimulated emission mechanism in these X-ray lines.

The group at the Naval Research Labs (ref. 14) have calculated that a quasistationary population inversion appears to be possible for elements with Z less than 40.

A particularly important experiment with supporting calculations has been reported at the University of Paris by Jaegle and co-workers (ref. 6). Computations of the population inversion for the inner shell electrons, as found in

aluminum, indicate a favorable transition from $2p^5 4d^3 P_1 \rightarrow 2p^6 1S_0$ line of Al^{3+} at 117.4 Å. Calculations concerning these intense line emissions indicate a high probability for population inversion from free electron excitation and a small probability for depopulation due to spontaneous radiation or non-radiative transitions. Their experiments with a 20J, 40 nsec, 1.06 μ laser show the 117.41 Å line of Al to be superradiant since it exhibits a negative absorption in the dense part of the laser plasma. Similar evidence of anomalous intensities and line narrowing has been reported by Peacock and Irons at Culham (ref. 11). Using a focused 1 GW Nd: glass laser on a polyethylene target they were able to show a population inversion in C^{5+} . In neither of these last two reports was X-ray lasing observed, due to insufficient inversion density; however, they provided encouraging experimental observations.

These results and calculations build a case for the X-ray lasing phenomenon only to the extent of being circumstantial evidence indicating that it might occur and not disproving the concept. A great deal of detailed theoretical physics remains to be accomplished. For example, cross sections and various lifetimes must be ascertained and multiple ionization, resonance charge exchange phenomena, auto-ionization, inner shell transitions, three body and dielectric recombination, and inner shell photoionization process must be more carefully studied.

Present knowledge has permitted a first order calculation; however, the theory now requires better numerical input to refine these calculations. What is needed is an inexpensive, carefully planned, preliminary experiment to determine the detailed character of the X-ray emission and to correlate it with accurate measurements of the emitting laser produced plasma. Depending on the results and analysis of this experiment, further modified experiments could be attempted as the need for more detailed inputs for calculations is established. During an experiment aimed at achieving X-ray laser action, other requisite information, such as instability heating and nonlinear plasma interactions, would become available from the ERDA-funded laser fusion program. The AFWL maintains constant and close liaison with the groups at LLL, LASL, NRL, the University of Rochester, and KMS Corporation.

The remainder of this report includes sections which cover supporting technical considerations, a possible experimental program, and a discussion of hard X-ray lasers. Section II discusses possible inversion schemes, quantitative aspects of the selected mode-locked laser approach, and a rough estimate of

the expected photon and energy losses. Section III discusses the laboratory equipment available for use, as well as the details of a possible experimental effort. A discussion of the status of hard X-ray lasers and an estimate of the power required for such devices is contained in section IV. Finally, this report is summarized in section V.

SECTION II

TECHNICAL CONSIDERATIONS

1. INTRODUCTION

In this section, the basic concepts for fabrication and investigation of an X-ray laser are discussed. The section begins with a listing of the general requirements for laser action in the soft X-ray range. Then three basic approaches for obtaining a population inversion at the appropriate frequencies are discussed in some detail.

2. GENERAL REQUIREMENTS FOR LASER ACTION

As in any laser concept, the gain coefficient (g) must exceed the loss coefficient (α) if amplification is to take place. For this to occur at the frequencies being considered, a large population inversion is required. Such a large population inversion requires that the excitation time (τ_{ex}) be short compared to the Auger time (τ_a) for the material. To ensure that the bulk of the excited ions actually participate in the lasing process rather than decaying spontaneously or reverting to another excited state, it will also be necessary for the stimulated emission time (τ_{st}) to be shorter than either the Auger or the spontaneous emission time (τ_{sp}). These fundamental requirements are summarized below:

$$\begin{aligned} g &\gg \alpha \\ \tau_{ex} &\ll \tau_a \\ \tau_{st} &\ll \tau_{sp} \\ \tau_{st} &\ll \tau_a \end{aligned}$$

3. POSSIBLE APPROACHES

Three proposed schemes for achieving the stripping (total ionization) of a sufficient number of atoms to yield significant inversion for a soft X-ray laser are discussed. They are:

(a) Use of relativistic electron beams to ionize a target material by direct electron impact.

(b) Use of ion beams and a thin film of target material to create an inversion through charge exchange mechanisms.

(c) Use of an extremely high power, mode-locked laser to produce a dense, high temperature plasma to yield the desired inversion.

There are numerous other approaches of some merit suggested by several individuals, e.g., Lubin (ref. 15), Duguay (ref. 16), Wood (ref. 17), etc., but they will not be treated here as they are either sufficiently different in process or involve difficult geometries.

4. ELECTRON BEAMS

The first general approach to creating a population inversion for an X-ray laser involves the use of relativistic electron beams to bombard a target material. The inversion results from inner electron shell vacancies created by direct electron impact.

Using 10 MeV electron beams and low Z targets such as carbon or beryllium, the electrons will penetrate to a depth on the order of 1 cm. Since such high energy beams can be focused to a spot on the order of 1 mm in diameter (ref. 6), the volume in question is 10^{-2} cm^3 . For a current of 10^6 amps, the power per unit volume is

$$p = \frac{(10 \text{ MeV/e}^{-1}) (10^6 \text{ amps})}{10^{-2} \text{ cm}^3} = 10^{15} \text{ watts/cm}^3 \quad (1)$$

As will become evident during the discussion of the mode-locked laser approach, this power density is considerably below that required for an X-ray laser. Also, since available electron beams are produced only in long pulses (10 to 100 nanoseconds) with relatively long risetimes and high energies, this method of excitation may not be suitable for the approach suggested in this paper.

5. ION BEAMS

There are two schemes involving the use of ion beams to create an inversion for an X-ray laser. The first scheme, proposed by McCorkle (ref. 18), involves creation of inner shell vacancies in the beam through ionizing collisions while the second scheme, proposed by Scully (ref. 19), involves electron pickup. The two schemes are discussed separately below.

a. McCorkle Scheme - In this scheme, ions of the desired material are used to bombard a thin metal foil. While being propelled through the foil with an

energy of $\approx 1 \frac{\text{keV}}{\text{amu}}$, the ions collide with the metallic atoms creating inner shell vacancies. The vacancies thus created lead to a population inversion in a very thin layer just above the foil. Using a deflection system, the ion beam can be swept along the foil at approximately the speed of light. Thus, in principle, a population inversion travelling with the wavefront of the emitted X rays can be created.

b. Scully Scheme - In this approach, a beam of completely stripped nuclei such as He^{+2} or Li^{+3} would be passed through a thin foil. The foil material and thickness would be chosen to maximize the probability of effecting charge pickup in an excited state. When the ions emerge on the other side of the foil, a population inversion between two states (i.e., the 2p and 1s for He^{+2}) would result. Travelling wave X-ray amplification would be effected by sweeping the ion beam along the foil at approximately the speed of light in a manner similar to that proposed in the McCorkle scheme (ref. 18).

Both of the above techniques are interesting and show some promise for the future, but at this date, they are only proposed schemes for obtaining a population inversion. Very extensive scientific and engineering efforts would be required to develop either of these pump excitation mechanisms.

6. MODE-LOCKED LASER

Using a moderate energy mode-locked laser to produce a dense, high temperature plasma appears to be the most promising approach for producing the inversion required for a soft X-ray laser. The essential features of this approach are discussed in some detail in the following paragraphs.

a. Power Analysis - If 10^{12} watts (at 1.06μ) is focused onto a target with a spot size of ~ 30 microns, the electric field, E , produced at the surface is $\sim 6 \times 10^9$ V/cm. This field is sufficient to produce rapid tunneling of the valence electrons into the conduction band separated by energy, ϵ_g , in a time

$$t = \sqrt{\frac{2m\epsilon_g}{eE}} \quad (2)$$

For $\epsilon_g = 10$ eV, the tunneling occurs in a time $t = 2 \times 10^{-17}$ sec. This produces a plasma of electron density $N_e \approx 10^{23}/\text{cm}^3$, which allows the electromagnetic field to penetrate to a depth of ≈ 0.3 micron. Within this layer, the electrons gain energy, ϵ , between electron-ion collisions ($\tau_c \approx 10^{-15}$ sec) given by

$$\epsilon = \frac{e^2 E^2}{M \omega^2} \approx 10^3 \text{ eV} \quad (3)$$

This energy is acquired in about the time needed for one-half of a cycle of the laser electromagnetic wave, which is much shorter than the time necessary for equilibration.

One can calculate the minimum laser power necessary to produce and maintain an inversion in a volume V . The power is given by

$$P = \frac{N_e V}{\tau_a} h_\omega \quad (4)$$

where $1/\tau_a$ is the Auger rate, taken as 10^{14} sec^{-1} . For $N_e = 10^{23}/\text{cm}^3$, $V = 3 \times 10^{-10} \text{ cm}^3$ and $h_\omega = 300 \text{ eV}$, the necessary laser power is $P = 10^{11} \text{ W}$. Thus high power, mode-locked Nd: glass lasers are capable of supplying sufficient power to achieve a population inversion within a focal volume of $3 \times 10^{-10} \text{ cm}^3$ ($\sim 3 \times 10^{20} \text{ W/cm}^3$).

To proceed further, we note that the excited states occupied by the electrons are Stark broadened. The broadening of the upper 2p state is approximately given by $\Delta \approx e^2 a N_e^{2/3}$, where N_e is the plasma electron density, e is the electron charge, and a is the radius of the 2p shell. In our case, $\Delta \approx 15 \text{ eV}$. Since the 1s state is not broadened as much as the 2p state, it appears as a relatively narrow state, which is nearly empty of electrons.

Although it is difficult to demonstrate the details of the inversion mechanism, Jaegle et al (ref. 6), using a Q-switched laser to bombard aluminum, have recently obtained "stimulated" emission at 117 \AA . However, the degree of inversion was not sufficient to achieve laser action. This implies that a higher level of excitation is required at this wavelength. In the following paragraphs, it will be shown that 10^{12} watts should be sufficient to produce the required inversion.

b. Gain Analysis - If laser action is to occur, the gain (g) must be sufficient to overcome photon losses (α). Furthermore, in a superradiant laser, the product of the net gain coefficient, $(g-\alpha)$, and the length of the active region, x , must be much greater than unity. The gain coefficient is given by

$$g = \frac{\lambda^2}{8\pi} \frac{\Delta N}{\Delta \nu} \frac{1}{\tau_{sp}} \quad (5)$$

where λ is the wavelength for the transition, $\Delta N \geq 10^{22}/\text{cm}^3$ is the number of ions inverted, $\Delta\nu \approx 10^{15} \text{ sec}^{-1}$ is the Stark broadened line width, and τ_{sp} is the spontaneous lifetime. The spontaneous lifetime is given by the expression

$$\tau_{\text{sp}} = \frac{1}{16\pi^2} \frac{h\lambda^3}{c^2 [\chi_{12}]^2} \quad (6)$$

where χ_{12} is the electric dipole element for the transition. For the $44 \text{ \AA } K_{\alpha}$ transition in carbon, $\tau_{\text{sp}} \approx 2.5 \times 10^{-12} \text{ sec}$. This time is much longer than either the tunneling time from equation 2 or the collision time, τ_c .

When these values are inserted into equations 5 and 6, the result is

$$g \approx 10^4 \text{ cm}^{-1} \quad (7)$$

c. Photon Losses - The photon loss mechanisms which must be considered are diffraction, Compton scattering, inverse Bremsstrahlung absorption, and photo-ionization. These mechanisms are discussed in the following paragraphs.

(1) Diffraction Losses - Diffraction effects are found to be significant for systems in which the wavelength of radiation is not negligible compared to the characteristic lengths of the system in question (ref. 20). Treating the system as a cavity with an exit aperture of 0.3μ , the ratio $\lambda/\ell = 117 \text{ \AA}/3000 \text{ \AA} \approx 0.04$. This ratio indicates that although diffraction loss may not be absolutely negligible, it will not be a fundamental loss mechanism for this effort.

(2) Compton Scattering - During the excitation and lasing process, the bulk of the electrons will be in unbound states. An estimate of the loss due to Compton scattering can be obtained by considering the electrons to be free electrons (subject to no potential). Under this assumption, the Klein-Nishina formula (ref. 21) for the total scattering cross section applies. However, for wavelengths on the order of 50 \AA , the cross section is very nearly equal to the Thompson cross section, which is $\sigma = 6.66 \times 10^{-29}$ (ref. 21). Then for a density of $10^{23} \text{ electrons/cm}^3$ and a length of 30μ , the collision probability per photon will be

$$\begin{aligned} P &= (6.66 \times 10^{-29} \text{ cm}^2) (10^{23} \text{ cm}^{-3}) (3.0 \times 10^{-3} \text{ cm}) \\ &= 1.98 \times 10^{-4} \end{aligned} \quad (8)$$

Even assuming that each scattered photon is lost, losses due to Compton scattering should thus be quite small ($\approx 0.02\%$).

(3) Inverse Bremsstrahlung Absorption - A third photon loss mechanism for an X-ray laser is inverse Bremsstrahlung absorption (absorption of a photon by a free electron). In cgs units, the absorption coefficient is given by (ref. 22)

$$\alpha_a = 3.69 \times 10^8 \frac{Z^3 N_i^2}{\nu^{3/2} T^{1/2}} \{1 - e^{-h\nu/kT}\} \quad (9)$$

Assuming $T = 10^6$ °K and $\lambda = 50$ Å, this is approximately

$$\alpha_a = 3.69 \times 10^8 \frac{Z^3 N_i^2 h}{\nu^{3/2} kT^{3/2}} \quad (10)$$

For the worst case, (complete ionization and $N_i = 1/6 N_e$),

$$\alpha_a = \frac{(3.69 \times 10^8) 6^3 (1/6)^2 \times 10^{46} (6.6 \times 10^{-34})}{(36 \times 10^{32}) (1.38 \times 10^{-23}) 10^9} \quad (11)$$

$$\alpha_a = 2.95 \times 10^2 \text{ cm}^{-1} \quad (12)$$

Inverse Bremsstrahlung absorption thus could be a significant loss mechanism for the X-ray laser using this approach.

(4) Photo-ionization - The final photon loss mechanism to be considered here is photo-ionization. This mechanism, which results in absorption of a photon and ejection of electrons from the absorbing material, constitutes a major portion of the absorption cross section at X-ray wavelengths. The cross section for inner shell ionization of carbon at 44 Å is $\sigma = 5 \times 10^{-24}$ (ref. 23). For $N_e = 1/6 \times 10^{23} \text{ cm}^{-3}$, the loss coefficient is

$$\alpha_a = (1/6 \times 10^{23}) (5 \times 10^{-24}) = 8.4 \times 10^2 \text{ cm}^{-1} \quad (13)$$

Photo-ionization should thus be the dominant photon loss mechanism in this effort. However, in actual operation, the loss due to photo-ionization should be significantly less than computed above as the plasma will be highly ionized for the bulk of the X-ray laser operation. Thus, few electrons should be in the bound 1s state.

(5) Total Photon Losses - Considering the two main photon loss mechanisms under worst case conditions, the total photon loss coefficient is approximately

$$\alpha_T = 8.40 \times 10^2 + 2.95 \times 10^2 = 1.135 \times 10^3 \text{ cm}^{-1} \quad (14)$$

$$\alpha_T = 11.4 \times 10^2 \text{ cm}^{-1} \quad (15)$$

d. Evaluation - This loss coefficient compares to a predicted (calculated) gain coefficient of 10^{+4} cm^{-1} (equation 7). Thus, the calculated gain coefficient is nearly an order of magnitude greater than the worst case loss coefficient. Using a conservative figure of $30 \mu\text{m}$ for the active length, the net gain is

$$(g - \alpha)x = (8.9 \times 10^3) (30 \times 10^{-4}) \approx 27 \quad (16)$$

which is much greater than unity. If x were made $\sim 100 \mu\text{m}$ or if the laser spot was made to sweep the target, a total gain-length product of over 100 is possible. The characteristic gain time is

$$\tau_3 = \frac{1}{(g - \alpha)c} = \frac{1}{(10 - 1.1) 10^3 (3 \times 10^{10})} \approx 3 \times 10^{-15} \text{ sec} \quad (17)$$

Fortunately, this time is shorter than both the Auger and spontaneous emission times. Based on the values computed for these critical parameters, it appears that a superradiant X-ray laser based on the laser produced plasma (mode-locked laser) approach is feasible.

7. SELECTION OF APPROACH

It is evident that a mode-locked laser is capable of producing a much higher power per unit volume than is obtainable using relativistic electron beams. In addition, details of any inversion scheme involving ion beams will require further analysis before they can be assessed. Since the initial calculations indicate that it is theoretically feasible, the mode-locked laser approach (or laser produced plasma approach) has been selected for this analysis. The target configuration, operational characteristics, and energy (pump) losses for such a device are discussed in the following paragraphs.

8. SOFT X-RAY LASER

a. Target Configuration - A Nd^{+3} : glass laser beam can be focused onto a bevelled carbon (diamond) or aluminum target as shown in figure 1. The laser beam, focused to an approximately $30\text{ }\mu\text{m}$ spot, will produce a blow-off plume which will travel mainly back in the direction of the incident laser beam. Although X rays will be emitted in all directions, superradiant emission should be favored in the regions nearest the sample as the electron density will be the highest in these regions. Furthermore, that direction orthogonal to both the laser beam and the target length should be most favored as in that direction there should be little or no cold plasma to act as an absorber (figure 1). This anisotropy of the emitted X-ray was recently observed experimentally (ref. 24).

A further possibility would be to produce a travelling wave excitation employing a cylindrical lens. This would enable one to compensate for propagation times which otherwise might allow for some deactivation before stimulated emission.

b. Operational Characteristic - The Nd : glass laser pulse duration will be on the order of 10 to 20 psec while the time for radiation to cross the $30\text{ }\mu$ spot is 10^{-13} second. This combination of pump and transit times would result in a laser operating in a pulsating mode. This pulsating mode is analogous to conventional mode (not Q-switched) operation for typical lasers. The output will consist of many (10 to 100) individual pulses spaced throughout the pumping pulse width.

For an inversion density of 10^{22} cm^{-3} (the factor of ten down from 10^{23} cm^{-3} takes into account the fact that not all ionized atoms will result in an inversion for the $2p-1s$ states) and a volume of $2 \times 10^{-10}\text{ cm}^3$, 2×10^{12} ions will be inverted. The energy per X-ray at $44\text{ }\text{\AA}$ is $E = 4.5 \times 10^{-17}$ joules. Then throughout a Nd^{+3} : glass laser pulse lasting 10 picoseconds, the power will be

$$P = \frac{(2 \times 10^{12})(4.5 \times 10^{-17})}{10^{-11}} = 9 \times 10^6 \approx 10^7 \text{ watts} \quad (18)$$

However, if 10 to 100 pulses occur during this 10 psec period, the peak power should be increased by a factor of 10 to 100, thus yielding a peak power of 10^8 to 10^9 watts. These powers correspond to X-ray laser to pump power efficiencies of 0.01% to 0.1%.

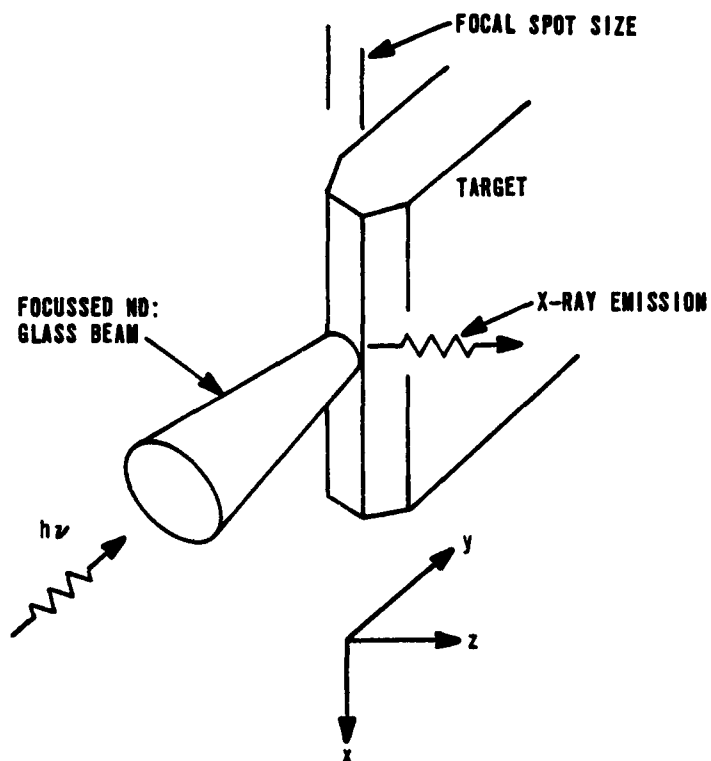


Figure 1. Schematic Diagram of Target Design and Orientation.

c. Energy Losses - The loss mechanisms to be discussed in this section are those which limit the energy which can be used to create the inversion (pump energy) but do not contribute to laser photon losses.

(1) Reflection Losses - Reflection losses, both prior to and after the formation of the plasma, will limit the energy which can be used to ionize the atoms in the target and accelerate the electrons. Although reflection losses have been observed to be as high as 40%, recent investigations, at KMS Fusion and the Lebedev Institute (ref. 25), indicate that target reflectivities decrease considerably (from their value under normal operating conditions) at power levels greater than 10^{12} to 10^{14} watts/cm². However, even if this decrease does not occur, reflection loss should not be a fundamental limitation in this effort.

(2) Hydrodynamic Loss - This loss results from pump power going into the motion of the plasma away from the carbon or aluminum target. Based on work done by the Livermore Group (ref. 17), the power loss due to hydrodynamic expansion is given by

$$P_h = \frac{VN_e kTC_s}{d} = AN_e kTC_s \quad (19)$$

when C_s is the speed of sound in the material. For the mode-locked laser approach, the hydrodynamic loss is estimated below.

$$P_h = \pi/4 (3 \times 10^{-5})^2 10^{23} (1.3 \times 10^{-23}) 10^6 \times 10^7 \quad (20)$$

$$P_h \approx 10^8 \text{ watts} \quad (21)$$

During the 10 picoseconds of interest (during the Nd: glass laser pump pulse), this corresponds to a total energy loss of 10^{-3} joule.

(3) Thermal Loss - Due to the high electron density and velocity expected for the laser produced plasma, thermal losses will be dominated by electrons. To obtain a worst case estimate of the electron thermal conduction loss, the plasma will be considered to be confined to a cylinder (of small aspect ratio) with one face adjacent to the target. For such an arrangement, the Livermore Group (ref. 17) estimates the power loss due to electronic thermal conduction to be given by

$$P_{\text{etc.}} = A \Sigma \nabla T \quad (22)$$

The temperature gradient can be approximated by $\nabla T = T/\ell$ where ℓ is the length of the cylinder. The electron thermal conduction coefficient (ref. 26) is

$$\Sigma = 20 (2/\pi)^{3/2} \frac{k^{7/2} T^{5/2}}{m_e^{1/2} e^4 Z \ln \Lambda} \quad (23)$$

where $\ln \Lambda$ is the coulomb logarithm for the plasma. Then

$$P_{\text{etc.}} = 10^3 A T/\ell \text{ watts} \quad (24)$$

where $\ln \Lambda$ has been extrapolated from tables (ref. 26) for $T = 10^6$ °K and $N_e = 10^{23} \text{ cm}^{-3}$. The power loss is approximately

$$P_{\text{etc.}} \approx 10^3 \left\{ 9\pi/4 \times 10^{-6} \right\} \frac{10^6}{3 \times 10^{-5}} \quad (25)$$

$$P_{\text{etc.}} \approx 2.36 \times 10^8 \text{ watts} \quad (26)$$

in the 10 picoseconds of interest (including both faces) the thermal energy loss is thus approximately

$$E_{\text{etc.}} \approx 5 \times 10^{-3} \text{ joule} \quad (27)$$

(4) Radiative Losses - In many dense high temperature plasmas, Bremsstrahlung losses are significant. A rough estimate of the Bremsstrahlung power density is given by (ref. 27)

$$P_r = 1.5 \times 10^{-38} Z^2 N_i N_e T^{1/2} \quad (28)$$

where T is in electron volts. Performing the computation, the result is

$$P_r = 9 \times 10^{15} \text{ watts/cm}^3 \quad (29)$$

based on the ionized volume of $V = 3 \times 10^{-10} \text{ cm}^3$, the total radiated power is

$$P = (9 \times 10^{15}) (3 \times 10^{-10}) = 2.7 \times 10^6 \text{ watts} \quad (30)$$

Thus, during the Nd^{+3} : glass laser pulse lasting 10^{-10} second, a total energy of

$$E = (2.7 \times 10^6) (10^{-11}) = 2.7 \times 10^{-5} \text{ joule} \quad (31)$$

will be lost due to Bremsstrahlung. For this application, therefore, Bremsstrahlung loss should not be significant.

In many applications, recombination radiation is considered as a significant energy loss mechanism. However, the recombination of electrons and ions plays a fundamental role in the inversion mechanism for this approach. As a result, recombination radiation will not be discussed as a loss mechanism in this report.

(5) Total Energy Loss - Excluding reflection losses, the total pump energy loss during the Nd : glass laser pulse should be less than 10^{-2} joule. Compared to the required output of several joules for the Nd : glass laser, an energy loss of 10^{-2} joule is not significant.

9. CONCLUSIONS

Based on the calculations presented in this section, it appears that a high power mode-locked laser is capable of producing an inversion sufficient to yield a gain which will dominate the photon losses. In addition, the energy pump losses associated with the X-ray laser described in this section will not be significant. Considering these quantitative estimates, the experimental verification of X-ray lasing described in the following section is feasible.

SECTION III

THE PROGRAM

1. INTRODUCTION

There are two basic phases of an experimental program for an X-ray laser effort: (1) verification of X-ray laser action and (2) investigation of the plasma/X-ray emission parameters pertinent to the operation of an X-ray laser.

2. VERIFICATION OF X-RAY LASER ACTION

Verification of X-ray laser action will be accomplished by the application and comparison of the results of a number of detection techniques. These techniques and the effects they are to detect are discussed in the following paragraphs.

a. Directional Effects - The first effect to be investigated is the directionality of X-ray emission. According to the theory discussed in Section II, the coherent X-radiation should be concentrated in the shape of a fan with the preferred emission direction being orthogonal to both the pump laser beam and the target length. This angular concentration of X-ray energy will be detected by a Channel Electron Multiplier Array (CEMA). A scintillator will then convert the output of the CEMA to an optical signal which is recorded on photographic film.

Commercially available (ref. 28) arrays consist of radiation sensitive elements (12 to 38 μ diameter, with a 15 to 53 μ center-to-center spacing) mounted over a total sensing area of 5 to 45 cm^2 . With these small individual sensing elements, the angular distribution of X-ray intensity can be accurately determined. Such accuracy will be essential if the directional effects characteristic of the X-ray laser emissions are to be detected.

b. Line-Narrowing - The second effect to be investigated is the wavelength narrowing of the X-ray transition which should accompany the onset of laser action. Since line-narrowing is characteristic of laser action, the line-width of emitted X-radiation should demonstrate a marked angular dependence as well. This angular dependence as well as the more usual temporal dependence of the expected line-narrowing will be monitored with a bent crystal spectrometer of AFWL design used in conjunction with a phosphor backed electron multiplier array

and photographic recording film. The vacuum chamber to be discussed in the next section is configured to allow simultaneous determination of the line-width and directional effects discussed in the two preceding paragraphs.

c. Threshold Effects - The presence of a gain threshold, characteristic of all lasers, will also indicate the onset of laser action. To observe this threshold, the output of the Nd^{+3} : glass pump laser will be varied over a broad range. The presence of a nonlinear increase in the X-ray output, as a function of input energy or power, would indicate the existence of a threshold.

d. Amplification Effects - The ability of the inverted atoms in the laser produced plasma to amplify small input signals of the appropriate frequency will be an important indicator of its ability to act as a medium to support super-radiant X-ray emission. To determine the amplification characteristics of the plasma, the input laser beam will be split into two beams. One portion of the beam will be used to excite a smaller target adjacent to the beveled slab (figure 2). Varying the time difference between the small signal source should enhance the output of the inverted region in the direction colinear with the small signal source and inverted region. This enhancement could be demonstrated with two detectors to measure the X-ray output both colinear with and orthogonal to a line connecting the two targets (figure 2). Proof of amplification can be achieved by varying the time delay between the two sources and looking for unequal intensities recorded by the two orthogonal detectors.

e. Coherence Effects - The presence of a high degree of spatial and temporal coherence in the emitted X-ray beam would be a strong indication that laser action was occurring. The degree of spatial coherence could be measured by determining the visibility of the fringes resulting from the interference produced by directing the beam through two coplanar pinholes. Similarly, the degree of temporal coherence could be measured by determining the visibility of the fringes produced when the beam is split and the two components are allowed to transverse different distances before they are recombined.

If the short temporal and small spatial extent of the beam do not make their analysis prohibitively difficult, these basic approaches will be used to determine the spatial and temporal coherence of the X-ray emission.

3. INVESTIGATION OF THE PLASMA/X-RAY PARAMETERS

The purpose of this report is not only to prove X-ray laser action feasible, but also to investigate the parameters of the laser produced plasma pertinent to

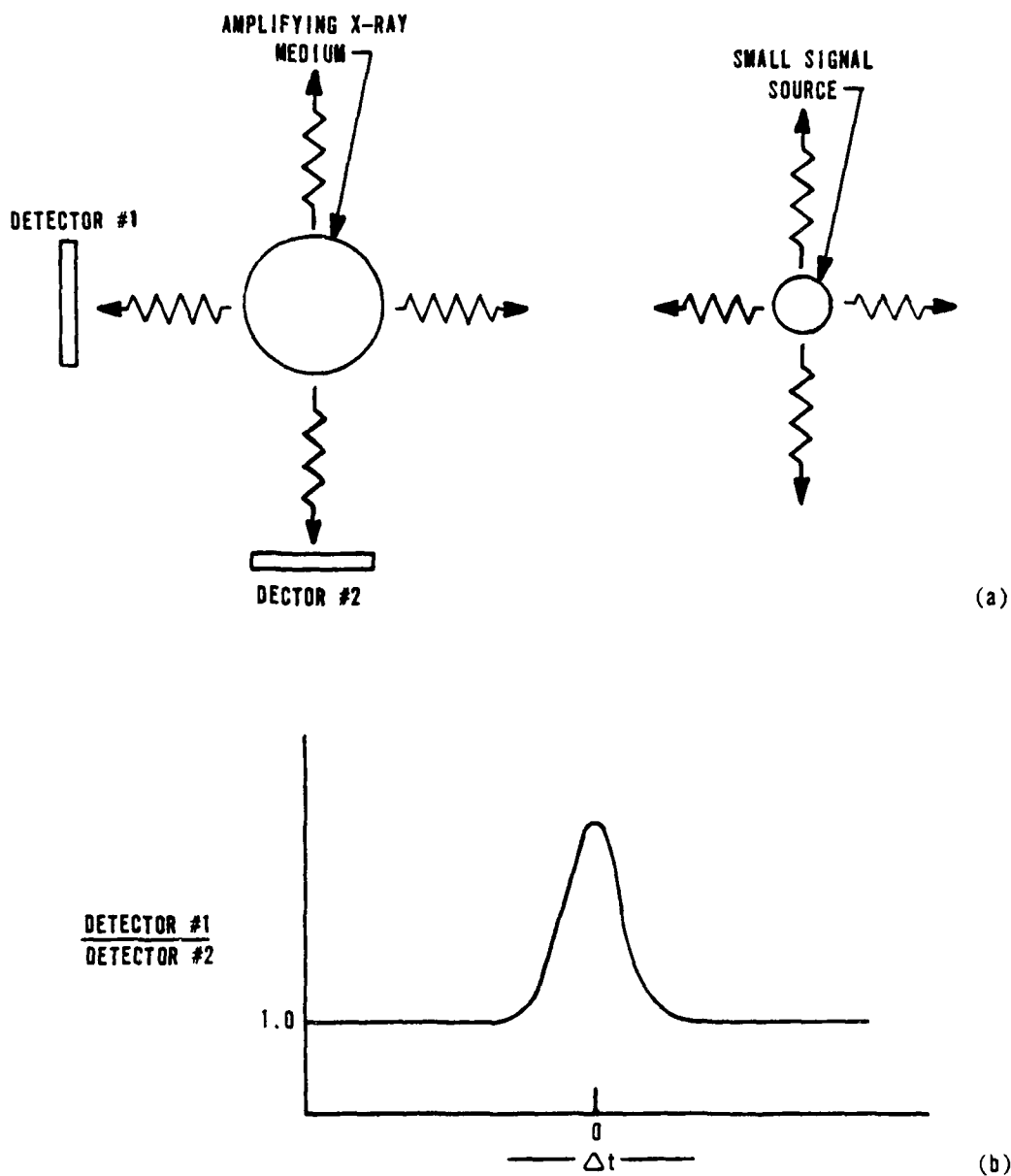


Figure 2. (a) Split-beam Excitation for Determining Laser Action.
 (b) Ratio of Detector of Signal No. 1 to Detector Signal No. 2 (ordinate) Versus Time Delay (abscissa) Between Split Laser Beams.

the efficient operation of such a device. A listing of some of the parameters to be measured is followed by a discussion of possible plasma and X-ray diagnostic techniques which can be employed to determine some of these parameters. Though these parameters are of vital importance for determining the exact nature of the X-ray lasing process, the feasibility program herein described would only be a follow up to an encouraging initial effort. The goal of an initial experimental effort will be to demonstrate the existence of X-ray lasing using a pulsed laser pump while the second phase will correlate X-ray laser action with plasma properties.

The plasma/X-ray laser parameters and effects to be measured or investigated in this effort include:

- (1) The electron and ion number densities.
- (2) The electron and ion temperatures.
- (3) The characteristic times for such mechanisms as spontaneous emission, Auger transitions, and complete ionization of the desired volume of the target material.
- (4) The recombination phenomenon which plays a crucial role in the proposed inversion mechanism.
- (5) The important photon and energy loss mechanisms.
- (6) The risetime, falltime, and pulsewidth of both the Nd⁺³: glass and X-ray lasers as well as their spatial intensity distributions.
- (7) The linewidth of the X-ray emission.
- (8) The effect of the atomic number of the target material on the inversion density.
- (9) The relationships between the X-ray and pump laser output energies and X-ray laser efficiency.
- (10) The effect of the target geometry on the X-ray laser gain and efficiency.
- (11) The effect of the character and amount of pump radiation reflected by the plasma on the degree of inversion achieved.

Where possible and when appropriate, these parameters and effects can be investigated on both a spatial and a time resolved basis.

Determining these parameters as well as others not listed will provide essential information in developing a detailed theory to describe the physics and operation of an X-ray laser. In addition, the information gained from these measurements will determine the directions taken in future X-ray laser investigations.

A large vacuum chamber and its associated observation ports to accommodate specific hardware will be the heart of the plasma/X-ray diagnostic system. The 36-inch diameter, 24-inch high stainless steel vessel is mounted over a large diffusion pump containing the necessary traps, controls, and valving to maintain a high vacuum. It is pumped via a base port and contains the necessary studs welded to the base to support a working table within the vessel.

The chamber contains a series of eight 4-inch ports (figures 3 and 4) located at the same level as the Nd: glass pump laser. One port (0°), to be fitted with a glass lens, will be used as the entrance port for focusing the pump laser beam. The 180° port will be used for the initial alignment and power monitoring of the Nd: glass laser beam. The 90° and 270° ports will serve as exit ports for detection and display of the X-ray laser pulse. At least one of the remaining ports will be used to display the output beam of the crystal spectrometer. The others may be used for an additional spectrometer, plasma diagnostics, or other X-ray detection devices. The ports at the lower level will provide access for electrical cables.

Within the chamber, a focusing lens, an xyz positioner (to properly position the target), and various plasma/X-ray diagnostic equipment will be mounted. The radiation models, to be used in conjunction with experimental measurements to describe the plasma, as well as the details of the plasma/X-ray diagnostics to be used with this chamber are discussed in the following paragraphs.

4. PLASMA/X-RAY DIAGNOSTICS

a. Radiation Models

(1) Line Radiation

In evaluating line radiation from a thermal plasma of known electron density and temperature, a collisional limit can be defined by (ref. 29)

$$N_e = 10^{12} (T_e)^{1/2} (\Delta E_{ki})^3 \text{ (cm}^{-3}\text{)} \quad (32)$$

where ΔE_{ki} is the energy level difference for a particular ionic species. For densities below this limit, radiative and collisional de-excitation are no longer balanced by their inverse process. In fact, for densities significantly below this limit, radiative de-excitation is much more dominant than collisional de-excitation.

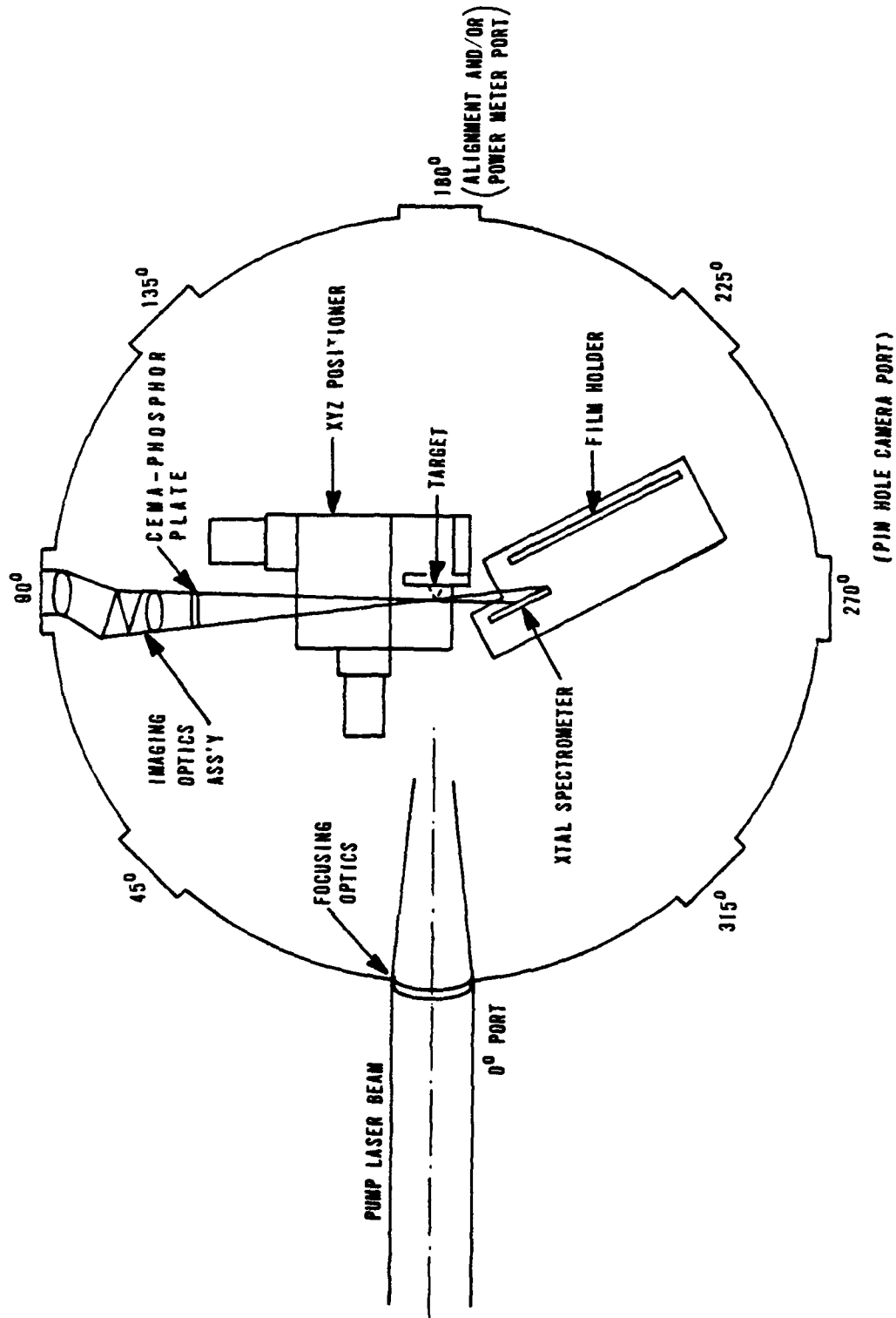


Figure 3. Schematic Drawing of Soft X-ray Laser Experimental Chamber.

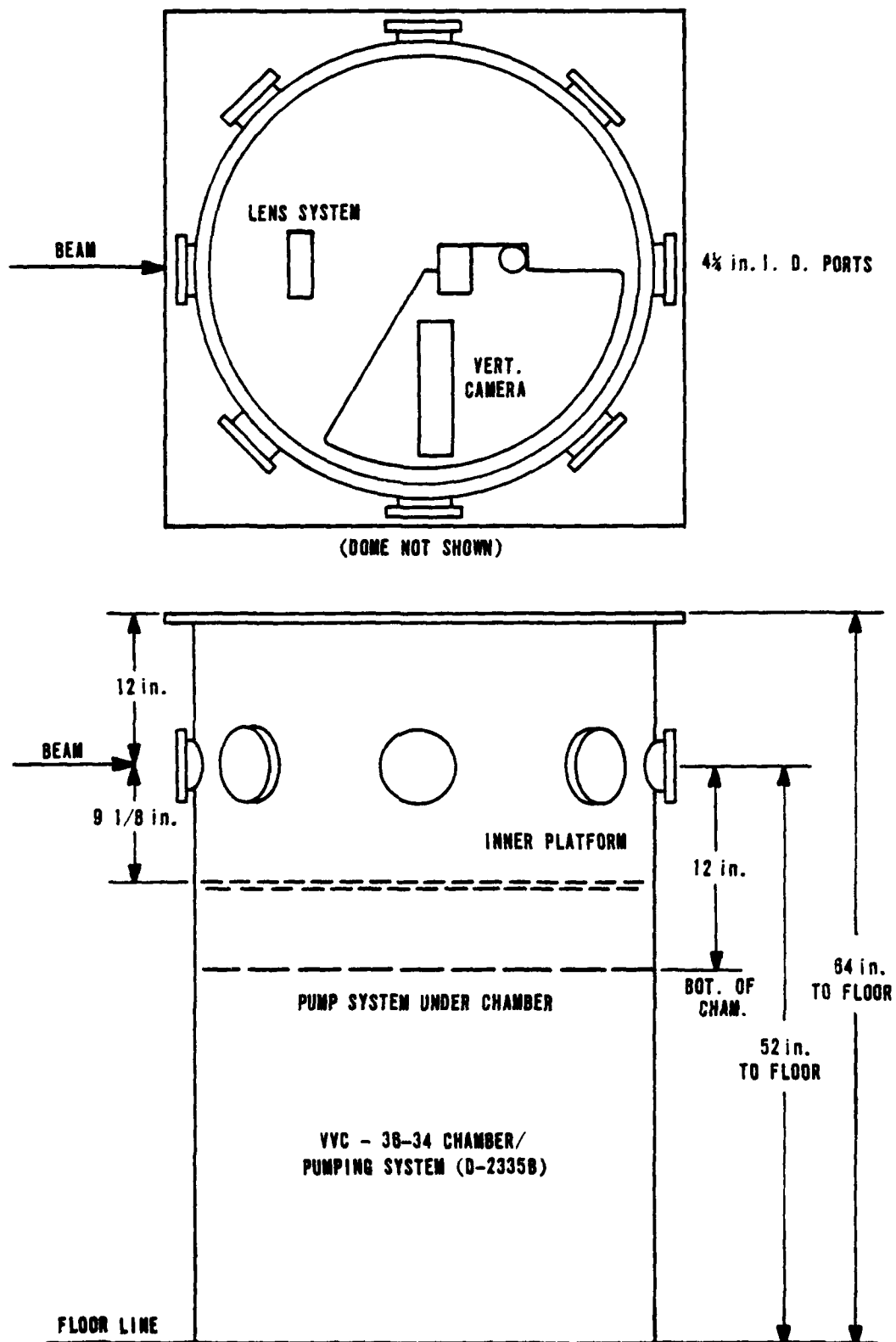


Figure 4. Sketch of Vacuum Chamber.

For a carbon plasma with a density of $N_e = 10^{22}/\text{cm}^3$ and $T_e = 10^6$ °K, only K_α and K_β type transitions from different ionic species would be below this limit. Therefore, the so-called corona equilibrium model could be applied to these states ($n=1, n=2$). At these temperatures and densities, line radiation is dominated by hydrogen-like and helium-like carbon (Carbon V, Carbon VI). By measuring the relative intensities between these two species and assuming a corona model, the electron temperature can be determined (ref. 26).

Alternately, within narrow temperature limits, the electron temperature could be obtained by determining the ratio between the satellite line (due to recombination) and the allowed transition intensities. A detailed exposition of the theory associated with this alternate approach is given in references 30 and 31.

Similarly, by measuring the broadened linewidth (from the Doppler or Stark effect), either the ion temperature or density can be determined if the relation between the ion and electron densities is known.

For Doppler broadened linewidths (ref. 26)

$$\Delta\lambda_D = 7.16 \times 10^{-7} \lambda_D (T_i/m)^{1/2} \quad (33)$$

For carbon plasma, assuming $T_i = 1$ keV, the resolution limit set on the Doppler effect is $\Delta\lambda_D/\lambda = 7 \times 10^{-4}$. A grazing incidence spectrograph would be marginal for this case.

However, for Stark broadened linewidths (ref. 32)

$$\Delta\lambda_S = 6 \times 10^{-11} n^{2/3} \frac{\lambda^2 k^2}{Z^*} \quad (34)$$

where Z^* is the effective charge of the emitting ions, $n = N_e + Z^{3/2} N_i$, and k denotes the Stark broadened quantum level. Again, for a carbon (V) plasma with $N_e = 10^{22}/\text{cm}^3$, $N_i = N_e$, $n = 1.47 \times 10^{23}$, $k = 2$ and $Z^* = 5$, the resolution limit set by the Stark effect is given by

$$\frac{\Delta\lambda_S}{\lambda_S} = 0.034 \quad (35)$$

This is on the borderline for a lead stearate diffraction crystal.

(2) Continuum Radiation

In the soft X-ray, vacuum ultraviolet regime with $T_i = 100$ eV and $N_e = 10^{22}/\text{cm}^3$, free-bound continuum radiation will dominate free-free continuum radiation. By measuring the relative intensities for free-bound transitions at two wavelengths, the electron temperature can be determined from (ref. 32)

$$KT = \frac{hc \left[\left(1/\lambda_2\right) - \left(1/\lambda_1\right) \right]}{\log \left[\lambda_1^2 \left[I_R(\lambda_1)/\lambda_2^2 \right] I_R(\lambda_2) \right]} \quad (36)$$

Outside the thermal plasma region where thick-target Bremsstrahlung due to "run-away" electrons may be important, the same relationship can be used to obtain a nonthermal temperature associated with this radiation (ref. 33).

b. X-ray Diagnostics

(1) Vertical Focusing Bragg X-ray Spectrograph

To maximize the utilization of the intensity arising from a point laser-plasma source, a method (due to von Hamos (ref. 34)) for the vertical focusing of a bent concave Bragg diffraction crystal will be adopted. It is analogous to the method of Johann (ref. 35) for horizontal focusing. However, instead of looking at a single wavelength as in the horizontal method, dispersion will be present in the horizontal plane (due to the width of the crystal). This method has recently been applied to a laser produced, iron plasma using a pyrolytic graphite crystal (ref. 22).

As lines associated with a carbon plasma are of primary interest, a lead stearate crystal with $2d = 100 \text{ \AA}$ has been chosen to examine the region from 20 \AA to 44 \AA . At 44 \AA , corresponding to a Bragg angle of 26° , the dispersion is 4.35 \AA/in. For a 2-inch wide crystal, this corresponds to a total dispersion of 8 \AA (ref. 36). The intensity of the vertical focusing crystal is approximately 5.8 times as great as that of a flat crystal.

The resolving power $\lambda/\Delta\lambda$ for lead stearate crystal has been measured for the carbon K_α line to be anywhere from 25 to 100 (ref. 37). To enable the measurement of line narrowing associated with X-ray laser action, the resolving power should fall in the high portion of this range. To determine the thermal plasma electron temperature, the free-bound continuum associated with C(V) and C(VI) will be recorded with the lead stearate, Bragg X-ray spectrograph described above.

The spectrograph can be rotated about the laser focal spot (that is, the laser produced plasma) without changing its wavelength range. Specifically, relative to the plane of the target surface, it can be rotated from $+30^\circ$ to -19° (where 0° is the surface of the target and the positive direction is in the direction of the laser, i.e., the laser is at $+90^\circ$). This rotational capability will allow the detection of directional effects associated with the laser-plasma or X-ray laser action.

The recording system for the spectrograph can be film. Ilford Q2 plates, which are linear between the optical densities of 0.1 and 0.3, will be used. These plates have been absolutely calibrated in intensity over this range of optical densities (ref. 38).

The entire crystal and film will be contained in a black anodized housing which shields against stray light. While firing, only the area to receive the range of Bragg defraction wavelengths will be visible on the crystal. The film plane will be shielded by a 1500 \AA aluminum filter to block out visible light and 1000 to 2000 \AA Parylene N filter to eliminate film fogging due to ultraviolet radiation.

(2) PIN Solid State Detector-Ross Filters Array

In the Ross filter technique (refs. 39 and 40), two similar detectors (e.g. doubly-diffused PIN silicon detectors) are placed behind a pair of X-ray absorbing foils of nearly the same atomic number. The thicknesses of the foils are adjusted to achieve matched transmission except in the energy range between their K-edges. As the sensitivity of the two filter-detector systems differs only in the region between their K-edges, the difference in their output signals will be proportional to the energy radiated in that region.

A set of 11 Ross filter pairs has been used to cover the energy range from 5 to 67 keV in the dense plasma focus. In a laser produced carbon plasma, radiation in this region should arise from thick target Bremsstrahlung as discussed earlier. If the temperature from the thermal portion of the laser plasma is in the few keV region, different thicknesses of beryllium foils will be used to determine an electron temperature based on radiation from the free-free continuum (ref. 33).

The most serious constraint on the use of such an array is the large solid angle required (approximately 4-inch for the array discussed above). The use of a large solid angle detector requires careful investigation for possible

source anisotropies. However, if there are good conversion from laser energy to X-ray energy and a high source strength, anisotropies can be neglected.

(3) Time-Resolved Pinhole Camera

A time-resolved pinhole camera consists of a pinhole aperture, a microchannel electron multiplier (ref. 41) with a rise time of ~ 2 nanoseconds, a 400 Å aluminum deposit on a fast plastic scintillator (rise time and decay time less than 1 nanosecond), and an image convertor camera. In the past, the need to capture as much light as possible has limited the spatial resolution obtainable with such time-resolved cameras. However, the increased efficiency of the electron multipliers has significantly reduced this problem. As a result, the spatial resolution is limited by the distance between adjacent microchannels, which is approximately 19μ (ref. 28).

Appropriate filters and this camera system can be used to discriminate against lower ionization states of carbon and to determine the spatial resolution of high ionization states, such as C(V) and C(VI). The result should yield an excellent measure of the spatial composition of the hot plasma volume.

(4) Other Diagnostics

Depending on the strength of the radiation source, other radiation diagnostics may be employed. These other radiation diagnostics might include a grazing incidence spectrograph (10 Å to 300 Å), ionization chambers ($< 300 \text{ Å}$), thermopiles (independent of λ), and X-ray diodes ($< 1000 \text{ Å}$).

The grazing incidence spectrograph is probably the most important of these standby diagnostics. The resolving power of this instrument, which is greater than 1000, will permit the determination of electron densities from Stark broadened line profiles. Also, resolution of satellite lines with this instrument will allow the plasma electron temperature to be determined. However, if this instrument is used, the vacuum chamber will have to be fitted to the entrance slit assembly of the spectrograph so that the plasma will only be a few millimeters from the entrance slits of the spectrograph.

SECTION IV

HARD X-RAY LASERS

1. INTRODUCTION

In this section, information concerning ideas and developments for a hard X-ray laser (≈ 10 keV) are briefly covered. The section includes discussions of the Utah experiment and general considerations for hard X-ray lasers.

2. THE UTAH EXPERIMENT

In July 1972, Kepros, Eyring, and Cagle (ref. 7) asserted that they had demonstrated the existence of a hard X-ray laser. Their assertion was based on the production of small spots on shielded X-ray film placed perpendicular to the focal line of a cylindrical condensing lens. The condensing lens was used to focus the output of a Nd: glass laser (30 joules in 20 nanoseconds) onto CuSO_4 gel sandwich to produce X-radiation.

The results of this experiment have been the object of considerable controversy. Despite isolated claims that the results of the Utah experiment have been reproduced, the claim that the existence of a hard X-ray laser has been demonstrated, has been largely discredited by numerous scientists (including some who originally supported the contention, as well as Siegenthaler (ref. 42), Boster (ref. 43), Rowley (ref. 44), and Lax and Guenther (ref. 1)). The claimed results have been discredited principally on the basis that the power density within the CuSO_4 gel target was not sufficient to generate X rays capable of producing the spots observed on the shielded film. In addition, the study by Boster (ref. 43) disputes the photographic evidence of X-ray lasing.

3. OTHER HARD X-RAY LASER CONSIDERATIONS

In their paper, Lax and Guenther (ref. 1) estimate that a laser power of 10^{15} watts would be required for the X-ray laser in the 10 keV region. They also point out that for such a laser, the lifetime for spontaneous emission is on the order of 10^{-15} second. This time is comparable to the stimulated emission and Auger transition times and is shorter than the thermalization time. Thus, unless the simulated emission time can be reduced and a laser of 10^{15} watts can be constructed, fabrication of a hard X-ray laser using the laser produced plasma approach may not be feasible.

Lax and Guenther also point out that it might be possible to construct a hard X-ray laser based on calculations by the Livermore group (ref. 17). These show that the density of a solid pellet can be increased by a factor of one-thousand by imploding the pellet with an array of lasers. Such a scheme would yield a stimulated lifetime of 10^{-16} second and would make construction of a hard X-ray laser a distinct possibility.

Based on the above considerations, realization of a hard X-ray laser may be sometime in the future. Fabrication of a soft X-ray laser (based on the mode-locked laser scheme proposed by Lax and Guenther) is possible with today's technology.

SECTION V

SUMMARY

1. CONCLUSIONS

Based on the discussion presented in Section IV, a significant advance in technology may be required before a hard X-ray laser is constructed and demonstrated. On the other hand, realization of a soft X-ray laser is possible relatively soon. The most promising approach for such a device is to use a high power, mode-locked laser to create a dense, high temperature plasma to generate the required population inversion. Based on the calculations contained in Section II of this report, an experimental demonstration of a soft X-ray laser using this approach can be accomplished in the near future.

To actually demonstrate the feasibility of fabricating a soft X-ray laser, the experimental program discussed in Section III of this proposal could be performed. Initially, the program would demonstrate the feasibility of fabrication an X-ray laser by this approach. In addition, it could establish the details of the inversion mechanisms as well as determine the X-ray laser parameters such as photon and energy losses, efficiency, energy output, and mode of operation.

2. FUTURE DIRECTIONS

The future directions pursued in this area would depend on the results obtained during the feasibility experiment discussed above. Should the initial attempts to produce a soft X-ray laser fail, the main thrust of an effort would be directed toward conducting a detailed plasma/X-ray analysis to determine the failings of the theory presented in Section II. Once determined, these failings would be remedied (if possible) by modifying the experimental apparatus.

However, once the feasibility of fabricating a soft X-ray laser has been demonstrated, there are three main directions open for future work. First, the specific device developed in this proposed effort could be improved. For example, various target materials and geometries could be tried to increase the efficiency and decrease the complexity of the device. The effect of lasers with specific pulse shapes to create the inversion to produce a hard X-ray laser could be investigated. This second direction involves the use of higher power

lasers ($> 10^{12}$ watts), possibly in conjunction with the implosion scheme proposed by the Livermore group. Since this effort involves the development of rather exotic technology, it may be several years in the future. Finally, a considerable effort to apply a developed X-ray laser to the large number of scientific areas discussed in Section I could be initiated.

The experimental program presented in this report involves difficult scientific and engineering problems. However, considering the theoretical basis for the program, it has an excellent probability of success.

REFERENCES

1. Lax, B., Guenther, A. H., "Feasibility of X-ray Lasers," Laser Interaction and Related Plasma Phenomena, Volume 3, Plenum Publishing Corporation, New York, pages 859-874, 1973.
2. Lax, B., Guenther, A. H., "Quantative Aspects of a Soft X-ray Laser," Applied Physics Letters, Volume 21, No. 8, pages 361-363, 15 October 1972.
3. Mallozzi, P. J., et al., "X-ray Emission From Laser Produced Plasmas," ARPA Order No. 1723, Battelle Columbus Laboratories, 28 January 1972.
4. Chapline, G., Wood, L., "X-Ray Lasers," Physics Today, pages 40-48, June 1975.
5. ARPA/NRL X-ray Laser Program, NRL Memorandum Report 3057, Naval Research Laboratory, May 1975.
6. Jaeglé, P., et al., "Superradiant Line in the Soft X-ray Range," Physical Review Letters, Volume 33, No. 18, pages 1070-1073, 28 October 1974.
7. Kepros, J. G., et al., "Experimental Evidence of an X-ray Laser," Proceedings of the National Academy of Science, Volume 69, No. 7, pages 1744-1745, July 1972.
8. Louisell, W. H., et al., "Analysis of a Soft X-ray Laser with Charge-Exchange Excitation," Physical Review A, Volume II, No. 3, pages 989-1000, March 1975.
9. Harris, S. E., "Generation of Vacuum-Ultraviolet and Soft X-ray Radiation Using High-Order Nonlinear Optical Polarizabilities," Physical Review Letters, Volume 31, No. 6, pages 341-344, 6 August 1973.
10. Basov, N. G., JETP Letters, Volume 5, page 141, 1967.
11. Irons, F. E., Peacock, N. J., "Experimental Evidence for Population Inversion in C^{5+} in an Expanding Laser-Produced Plasma," Journal of Physics, B, Volume 7, No. 9, pages 1109-1112, 21 June 1974.
12. Mallozzi, P. J., "Laser Plus Iron Target: Broad-Band X-ray Source," Physics Today, page 20, January 1972.
13. Mead, S. W., et al., "Preliminary Measurements of X-ray and Neutron Emission from Laser Produced Plasmas," Applied Optics, Volume II, No. 2, pages 345-352, February 1972.
14. Elton, R. C., Analysis of X-ray Laser Approaches: 2. Quasistationary Inversion on K-Alpha Inner Shell Transitions, NRL Memorandum Report 2906, Naval Research Laboratory, October 1974.

REFERENCES (Continued)

15. Bristow, T. L., et al., Optics Communications, Volume 5, page 317, 1972.
16. Duguay, M. A., and Rentzepis, P. M., "Some Approaches to Vacuum UV and X-ray Lasers," Applied Physics Letters, Volume 10, pages 350-352, 15 June 1967.
17. Slutz, S., et al., X-ray Lasers: Necessary Conditions and Some Possible Approaches, Cot/Phys 73-9, Lawrence Livermore Laboratory, 25 May 1973.
18. McCorkle, R. A., and Joyce, J. M., "Threshold Conditions for Amplified Spontaneous Emission of X-Radiation," Physical Review, A, Volume 10, No. 3, pages 903-912, September 1974.
19. Louisell, W. H., et al., "Analysis of a Soft X-ray Laser with Charge-Exchange Excitation," Physical Review, A, Volume 11, No. 3, pages 989-1000, March 1975.
20. Born, M., and Wolf, E., Principles of Optics, Pergamon Press, Oxford, 1975.
21. Leighton, R. B., Principles of Modern Physics, McGraw-Hill Book Company, Inc., New York, 1959.
22. Ready, J. J., Effects of High Power Laser Radiation, Academic Press, New York, 1971.
23. Henke, B. L., Measurement of Inner Shell Ionization Cross Sections, AFOSR TR-72-1140, April 1972.
24. Krokhin, O. N., et al., "Anisotropy of X-rays From a Laser Plasma," JETP Letters, Volume 20, No. 4, pages 105-107, 20 August 1974.
25. It has been reported by G. V. Sklizkov and others that the plasma reflectivity decreases quite dramatically at high laser intensity.
26. Stamper, J. A., et al., "Laser-Matter Interaction Studies at NRL," Third Workshop on Laser Interactions and Related Plasma Phenomena, RPI, August 13-17, 1973.
27. Tannenbaum, S. B., Plasma Physics, McGraw-Hill Book Company, Inc., New York, 1967.
28. Galileo Electro-Optics Corporation, Data Sheet 6300.
29. McWhirter, R. W. P., Plasma Diagnostic Techniques, Edited by Huddleston and Leonard, Academy Press, New York, 1965.

REFERENCES (Continued)

30. Gabriel, A. H., and Jordan, C., Case Studies in Atomic Collision Physics, Volume 2, Edited by McDaniel and McDowell, North Holland Publications, 1971.
31. Peacock, N. J., et al., "Satellite Spectra for Helium-Line Ions in Laser-Produced Plasmas," Journal of Physics, B, Volume 6, pages L298-L304, October 1973.
32. Conrads, H., "Diagnostics of High-Temperature, High Density Plasma by Radiation Analysis," Applied Spectroscopy Reviews, Volume 6, No. 2, pages 135-188, 1972.
33. Elton, R. C., NRL Report 6738, Naval Research Laboratory, 1968.
34. vonHamos, L., Annals of Physics, Volume 17, No. 6, pages 716-724, 1933.
35. Johann, H. H., Z Phys, Volume 69, # 3/4 pp 185-206, 1931.
36. Blakhin, M. A., Methods of X-ray Spectroscopic Research, Pergamon Press, Oxford, 1965.
37. Henke, B. L., Advances in X-ray Analysis, Volume 13, Plenum Publishing Corporation, New York, 1969.
38. Hobby, M. G., and Peacock, N. J., Spectrographic Calibration at Soft X-ray Wavelengths, Culham Laboratory, 1972.
39. Johnson, David J., "A Study of the X-ray Production Mechanism of a Dense Plasma Focus," Journal of Applied Physics, Volume 45, No. 3, pages 1147-1153, March 1974.
40. Johnson, D. J., Time Resolved X-ray Spectral Measurement System, AFWL-TR-72-40, Air Force Weapons Laboratory, Kirtland AFB, New Mexico, May 1972.
41. Bettinali, L., et al., "Soft X-ray Image Intensifiers with High Time and Space Resolution," Reviews of Scientific Instruments, Volume 42, No. 12, page 1834, December 1971.
42. Siegenthaler, K. E., et al., "Further Observations Relating to X-ray Laser Emission from CuSO_4 Doped Gelatin," Applied Optics, Volume 12, No. 9, page 2005, September 1973.
43. Boster, T. A., "Some Questions on the Evidence of Laser X-ray Emission From CuSO_4 Doped Gelatin," Applied Optics, Volume 12, No. 2, page 433, February 1973.
44. Rowley, P. D., and Billman, K. W., "Experimental Attempts to Confirm X-ray Lasing from CuSO_4 ," Applied Optics, Volume 13, No. 3, pages 453-455, March 1974.